XVIII IMEKO WORLD CONGRESS
Metrology for a Sustainable Development
September, 17 – 22, 2006, Rio de Janeiro, Brazil

UNCERTAINTIES OF MULTI SENSORS CMM MEASUREMENTS APPLIED TO HIGH QUALITY SURFACES

Jean Marc Linares [1], *Jean Mailhé* [2], *Jean Michel Sprauel* [3]

[1] CIME/EA(MS)², Aix en Provence, France, linares@iut.univ-aix.fr
[2] CIME/EA(MS)², Aix en Provence, France, mailhe@iut.univ-aix.fr
[3] CIME/EA(MS)², Aix en Provence, France, sprauel@iut.univ-aix.fr

Abstract: A statistical approach, based on a maximum likelihood criterion, is used to define the uncertainties of the derived element associated to a set of measured coordinates. The method is applied to high quality surfaces of low extent.

Keywords: Uncertainties, Measurement.

1. INTRODUCTION

Coordinate Measuring Machines (CMM) have brought a significant enhancement of industrial control practices. It has allowed accessing to larger information than with classical metrology approaches. But, at the opposite of this last one, the CMM cannot measure directly the geometrical dimensions corresponding to the ISO or ANSI geometrical specifications, of the part. In fact, the acquisition of the surfaces results in a series of set of points. Each set of points represents a sample of the surface where it has been probed. However, it contains both information about the spatial localization of the surface and its intrinsic geometrical characteristics. Different research programs were started last years [1] concerning the control of uncertainties in the whole industrialization process of a mechanical assembly. A generalized principle of uncertainty was thus presented [2]. In this topic the uncertainty of measurement is also considered. The concept of uncertainty is well-known in metrology. It is represented by a statistical parameter associated to the result of a given measurement. Uncertainties are related to the fact that each measurement is altered by random errors. These errors have to be quantified and reported in all the results or operations which derive from the measurement process. The studies carried out to define the uncertainties of CMM measurements can be sorted into three classes:

- Methods based on the use of calibrated parts: results of repeated experiments are compared to calibrated values of a user defined gauge. Systematic measurement deviations and random uncertainties of the features to be qualified are then derived from the calibration data base [3], [4].
- Simulations of the measurement process: A Monte Carlo Method (MCM) is commonly used to simulate a complex measurement process. It is an elegant alternative for treating complex measurements of dimensions and predicting the probability density distribution of acquired quantities [5].
- Statistical approaches: Least squares and extreme fits are commonly employed in CMM measurements. Numerous algorithms have thus been developed to perform three dimensional data analysis. Kurfess and Banks also developed a statistical approach to check the validity of geometrical models [6]. Yau proposed an evaluation method of the uncertainties of vectorial tolerances using a least squares optimization [7]. A linear approximation of the rotation and translation vectors of the surface, combined in a homogeneous coordinate transformation matrix was however used in this approach. Numerous studies of a set of measured points were also carried out by Henke and Summerhays. These authors suggest methods for evaluating the geometric errors of parts obtained with well defined manufacturing processes [8].

In our paper, a maximum likelihood criterion will be used to estimate the uncertainties of the parameters of the derived element associated to a set of coordinates. The method will be applied to surfaces of high quality and low extent where the distribution of the points around the mean surface can be assumed to be Gaussian. To demonstrate the effect of uncertainty propagation in the best fit, the case of a distance between a straight line and a point will be first considered. The impact of geometrical constructions will be then illustrated using the case of 3D line constructions.

2. EXPERIMENTAL DETERMINATION OF THE SIGNATURE

Acquired coordinates include the texture of the analyzed surface, called manufacturing signature, and the deviations of the CMM sensor named measurement signature.

2.1. Manufacturing signature

Surface generation imposes the trace of the cutting tool to the matter, depending on the shape of the cutting edges and the machining paths (turning, milling…). This trace is the manufacturing signature.

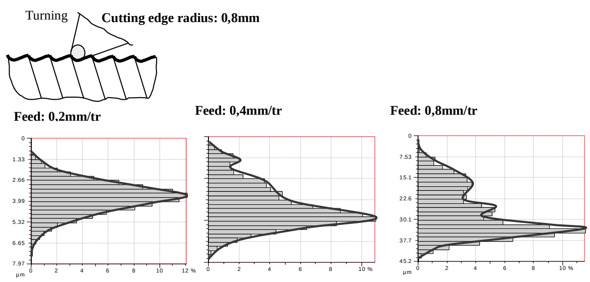

Fig.1. Turning signature

In the case of turning, the signature imposed to the surface varies according to the cutting parameters, the cutting edge geometry and some uncontrolled parameters (vibration, metal shearing, wrenching…). The signature probability densities of three cylinders turned with a cutting edge radius of 0.8 mm and three longitudinal feeds (0.1 - 0.2 and 0.4 mm/rev), are presented in figure 1. With fine feed, the random phenomena are larger than the systematic effects imposed by the cutting edge geometry. The probability density becomes symmetrical and tends to a Gaussian distribution. On the contrary, the dissymmetry of the density probability increases when the trace of the tool becomes more significant. These conclusions can be generalized to milling. In grinding, however, each grain of abrasive forms a cutting edge, thus leading to random cutting.

2.2. Measurement signature

Measured values are disturbed by the acquisition realized by the measuring machine. The geometrical defects, the repeatability... of the measuring machine are included in the coordinates of the measured points. The measurement signature is represented by these defects. In a measurement of a surface with small extent, the density of probability of the signature of the coordinate measuring machines (CMM) has a range between 2.5 µm and 6 µm. The signatures of new measurement processes without contact are lower (MOS of MAHR, Micromesure 2 of STIL…). Figure 2 shows the probability density of the signature of such last optical CMM. It is obtained by measuring a glass gauge using normal conditions of operation. Its range is 0.137 µm. When the geometry of the machine is of good quality or its defects accurately corrected, the probability density of the measurement signature is symmetrical and fits to a Gaussian.

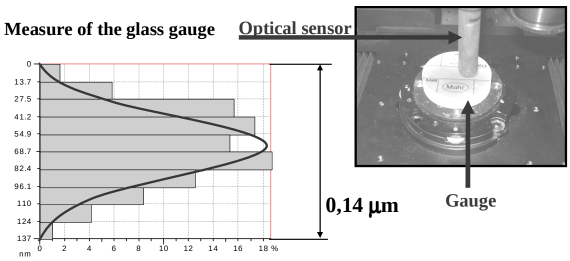

Fig.2. Measurement signature

3. DETERMINATION OF UNCERTAINTIES

3.1. Likelihood method and uncertainty propagation

The combined signature is the convolution of the manufacturing and measurement signatures. For surfaces of high quality, the measurement signature has a predominant influence on the combined signature (figure 3). The best fit of the analyzed surface should therefore use a least squares optimization. In fact, this criterion assumes a Gaussian distribution of the residues around the derived surface, which is in agreement with the previous combined signature.

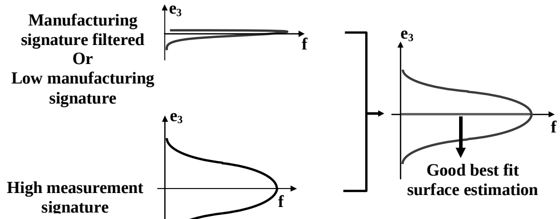

Fig.3. Measurement signature

The likelihood function ϕ of the least squares optimization criterion is:

$$\phi = \left[\frac{1}{\sigma\sqrt{2\pi}}\right]^N \mathrm{Exp}\left[-\frac{1}{2}\sum_{k=1}^{N}\left(\frac{\delta_k}{\sigma}\right)^2\right] \quad (1)$$

The best-unbiased estimators a_i of the parameters a_i defining the fitted surface are thus derived from the following optimization conditions:

$$\frac{\partial\phi}{\partial a_i} = 0 \Rightarrow \sum_{k=1}^{N}\delta_k\frac{\partial\delta_k}{\partial a_i} = 0 \quad (2)$$

If the p parameters a_i of the geometric element associated to the digitized surface were perfectly defined, the standard deviation σ could also be estimated in the same way:

$$\frac{\partial\varphi}{\partial\hat{\sigma}} = 0 \Rightarrow \hat{\sigma} = \sqrt{\frac{1}{N}\sum_{k=1}^{N}\delta_k^2} \quad (3)$$

However, such estimator would lead to a biased evaluation of σ, because a set of p parameters a_i has already been derived from the acquired data. Therefore, the standard deviation of the measurement has to be computed with the following expression, also called residue of the least squares optimization:

$$\hat{\sigma} = \sqrt{\frac{1}{N-P}\sum_{k=1}^{N}\delta_k^2} \quad (4)$$

This deviation $\hat{\sigma}$ can be propagated to deduce the covariance matrix of the estimated parameters a_i, using equation (2) and classical differential expressions of the uncertainties. From the diagonal components of the covariance matrix, the error bars of a_i are then easily calculated, since the statistical distribution of these random variables corresponds to a Fisher-Student law. Moreover, the covariance matrix is also useful to propagate the uncertainties of the fitted surfaces to any derived geometric element. It has to be pointed out that the propagation process of the standard deviation $\hat{\sigma}$ requires a precise definition of the derivatives $\partial\delta_k/\partial\hat{a}_i$. It allows processing all the classical surfaces, i.e. lines, planes...

To simplify the demonstration of the propagation of uncertainties in the control of geometrical specifications, the case of the distance between a point and a straight line in a

2D plane will be considered. It will be possible then to generalize the conclusions to any 3D problem.

3.2. Uncertainty of the best fit line

To illustrate the approach, the case of a 2D straight line will be considered for its simplicity.

3.2.1. Statistical model

The coordinates y_k of the measured points are all assumed to be independent and have the same uncertainty. Their distribution follows a Gaussian law with a variance equal to σ^2. The coordinates x_k are supposed to be certain. The occurrence probability of given coordinates (x,y) to belong to the 2D straight line defined by its intercepts a_0 and its slope a_1 can be written as follows [9]:

$$f(y)=\frac{1}{\sigma\sqrt{2\Pi}}e^{-\frac{1}{2}\left(\frac{y-(a_0+a_1.x)}{\sigma}\right)^2} \quad (5)$$

The conditional probability that the whole set of measured coordinates (x_k,y_k) belongs to the straight line, is provided by the product:

$$\phi(y_1,y_2,\ldots,y_N)=\prod_{k=1}^{N}f(y_k)=\left(\frac{1}{\sigma\sqrt{2\Pi}}\right)^N e^{-\frac{1}{2}\sum_{k=1}^{N}\left(\frac{y_k-(a_0+a_1.x_k)}{\sigma}\right)^2} \quad (6)$$

The maximization of this likelihood function will be obtained by the minimization of the following function depending on the parameters of the random vector **a** (a_0,a_1):

$$\max\left(\prod_{k=1}^{N}f(y_k)\right)=\min\left(-\frac{1}{2}\sum_{k=1}^{N}\left(\frac{y_k-(a_0+a_1.x_k)}{\sigma}\right)^2\right) \quad (7)$$

To calculate of the mean values (first order moment) of the random vector **a,** let us introduce the following function W:

$$W=-\frac{1}{2\sigma^2}\sum(y_k-(a_0+a_1x_k))^2 \quad (8)$$

The parameters of the random vector **a** are thus calculated by the resolution of the minimization conditions (9):

$$\frac{\partial W}{\partial a_0}=0 \quad \text{and} \quad \frac{\partial W}{\partial a_1}=0 \quad (9)$$

The best linear unbiased estimation of the parameters **a** of the straight line becomes thus:

$$a=\begin{pmatrix}a_0\\a_1\end{pmatrix}=\frac{1}{N\sum x^2{}_k-(\sum x_k)^2}\times\begin{pmatrix}\sum x^2{}_k\sum y_k-\sum x_k\sum x_k.y_k\\ N\sum x_k.y_k-\sum x_k\sum y_k\end{pmatrix} \quad (10)$$

The variances and covariance of a_0 and a_1 are derived then from equation (3), using classical propagation equations. The variance of the intercept a_0 is defined by the following calculations (11):

$$var(a_0)=\sum_{k=1}^{N}\left(\frac{\partial a_0}{\partial y_k}\right)^2.var(y_k)+2\sum_{k=1}^{N-1}\left(\frac{\partial a_0}{\partial y_k}\right).\sum_{j=k+1}^{N}\left(\frac{\partial a_0}{\partial y_j}\right).cov(y_k,y_j) \quad (11)$$

$$var(a_0)=\sum\left(\frac{\partial a_0}{\partial y_k}\right)^2.var(y_k) \text{ with } \left(\frac{\partial a_0}{\partial y}\right)=\frac{\sum x^2-\sum x.x_k}{N\sum x^2-(\sum x)^2}$$

$$var(a_0)=\frac{\sum x^2}{N\sum x^2-(\sum x)^2}.var(y_k)=var(a_0)=\frac{\sum x^2}{N\sum x^2-(\sum x)^2}.\sigma^2$$

The variance of the slope a_1 is obtained through subsequent derivations (12):

$$var(a_1)=\sum_{k=1}^{N}\left(\frac{\partial a_1}{\partial y_k}\right)^2.var(y_k)+2\sum_{k=1}^{N-1}\left(\frac{\partial a_1}{\partial y_k}\right).\sum_{j=k+1}^{N}\left(\frac{\partial a_1}{\partial y_j}\right).cov(y_k,y_j) \quad (12)$$

$$var(a_1)=\sum\left(\frac{\partial a_1}{\partial y_k}\right)^2.var(y_k) \text{ with } \left(\frac{\partial a_1}{\partial y}\right)=\frac{N.x_k-\sum x_k}{N\sum x_k{}^2-(\sum x_k)^2}$$

$$var(a_1)=\frac{N}{N\sum x_k{}^2-(\sum x_k)^2}.var(y_k)=\frac{N}{N\sum x_k{}^2-(\sum x_k)^2}.\sigma^2$$

The covariance between a_0 and a_1 is deduced from the same kind of computation (13):

$$cov(a_0,a_1)=\sum_{k=1}^{N}\left(\frac{\partial a_0}{\partial y_k}\right)\left(\frac{\partial a_1}{\partial y_k}\right).var(y_k) \quad (13)$$

$$cov(a_0,a_1)=\frac{-\sum x_k}{N\sum x_k{}^2-(\sum x_k)^2}.var(y_k)=\frac{-\sum x_k}{N\sum x_k{}^2-(\sum x_k)^2}.\sigma^2$$

These results can be gathered in the following matrix expression (14):

$$Cov(\mathbf{a})=\frac{\sigma_p{}^2}{N\sum x_k{}^2-(\sum x_k)^2}\times\begin{pmatrix}\sum x_k{}^2 & -\sum x_k\\ -\sum x_k & N\end{pmatrix} \quad (14)$$

In metrology field, the parameters a_0 and a_1 are transformed to geometrical parameters such as the direction vector **V** of the straight line and a point **C** of the feature (figure 4). Generally, point **C** is defined by the center of gravity of the measured points. The variance covariance matrix of these geometrical parameters is calculated using the classical propagation equation.

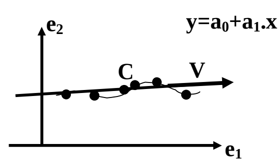

Fig.4. Statistical variables to the vectorial variables

For a straight line, the variance covariance matrix of **C** and **V** is obtained by introducing the following Jacobian transformation (15):

$$\mathrm{Cov}(\mathbf{C},\mathbf{V}) = J_{(\mathbf{C},\mathbf{V})}.\mathrm{Cov}(\mathbf{a}).J^{t}_{(\mathbf{C},\mathbf{V})}$$
$$\mathbf{C}\left|\begin{matrix}0\\ a_0\end{matrix}\right. \qquad \mathbf{V} = \frac{1}{\sqrt{1+a_1^2}}.\left|\begin{matrix}1\\ a_1\end{matrix}\right. \tag{15}$$

The Jacobian matrix J is defined by equation (16):

$$J^{t}(\mathbf{C},\mathbf{V}) = \begin{pmatrix} \frac{\partial C_x}{\partial a_0} & \frac{\partial C_y}{\partial a_0} & \frac{\partial V_x}{\partial a_0} & \frac{\partial V_y}{\partial a_0} \\ \frac{\partial C_x}{\partial a_1} & \frac{\partial C_y}{\partial a_1} & \frac{\partial V_x}{\partial a_1} & \frac{\partial V_y}{\partial a_1} \end{pmatrix} \tag{16}$$

3.2.2 Error bar of the straight line

The knowledge of the variance covariance matrix permits to define, at any point of the line, the uncertainty in a fixed direction characterized its normal vector **n** (figure 5). As example, a normal vector collinear with the second axis e_2 is considered. The error bar obtained for a given level of risk α is defined by the following calculations:

$$\begin{aligned} &\mathrm{var}(y) = J(y).\mathrm{Cov}(a).J^{t}(y) \quad \text{with} \quad J(y) = \begin{pmatrix}1 & X\end{pmatrix} \\ &\mathrm{var}(y) = \mathrm{var}(a_0) + 2.X.\mathrm{cov}(a_0, a_1) + X^2.\mathrm{var}(a_1) \\ &U = k(\alpha).\sqrt{\mathrm{var}(y)} \end{aligned} \tag{17}$$

The variance of y_k (σ_p^2) is estimated by the residue of the least squares:

$$\sigma_p^{\,2} = \frac{1}{N-2}.\sum\left(y_k - (a_0 + a_1.x_k\right)^2 \tag{18}$$

Using equation (17), the error bar of the straight line can be plotted. This envelope depends on the level of risk α assumed in the calculations.

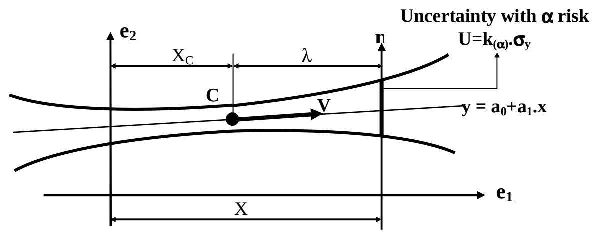

Fig.5. Line error bar

The lowest uncertainty is obtained when the given point is close to the center of gravity **C** of the measured coordinates (figure 5). λ is the distance between the estimation point and the **C**. The more the value of the variable λ increases the more the error bar grows.

3.2.3 Rules for geometrical element measurement

The study of this error bar model permits to reduce the propagation uncertainty. Equation (19) gives the variance covariance matrix when the origin of the coordinate system is shifted to the center of gravity **C**. This matrix is diagonal. It means that the covariance $\mathrm{cov}(a_0,a_1)$ is equal to zero.

$$a_i = \begin{pmatrix} \frac{\sum y_k}{N} \\ \frac{\sum x_k.y_k}{\sum x^2_k} \end{pmatrix} \quad \mathrm{Cov}(a_i) = \begin{pmatrix} \frac{\sigma_p^{\,2}}{N} & 0 \\ 0 & \frac{\sigma_p^{\,2}}{\sum x^2_k} \end{pmatrix} \tag{19}$$

The uncertainty of the constant parameter (a_0) is mainly influenced by the number of acquired points. Figure 6 represents the experimental uncertainty of the radius of a circular gauge measured by a classical CMM. When the statistical effect is preponderant in the measurement process, a reliable estimation of the surface parameter uncertainties requires a number of measured points greater than three times the number of parameters describing the analyzed surface. In the case of a circle case, for example, this last number is 3 (two translations and a radius) in consequence, the minimal number of measured points is 3 x 3 = 9 points.

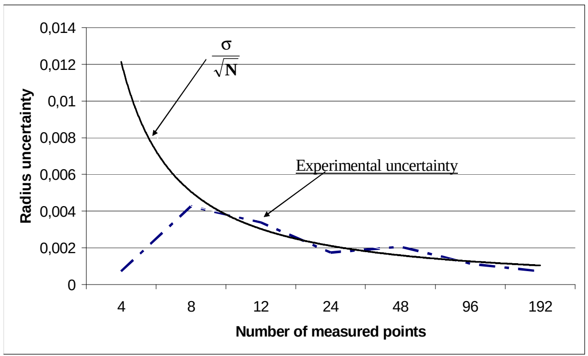

Fig.6. Measured point number

This remark is validated by figure 6. When the number of measured points is less than 9, the estimated uncertainty is incorrect. The minimal number required for measurement of classical surfaces is proposed in table 1.

Table.1. Minimal number of the measured points

3D Line	Plane	Circle	Cylinder	Cone	Sphere
12	9	9	15	18	12

The error bar of the slope a_1 depends also on the measurement extent X, and the number of points N. The minimal uncertainty will be reached, thus, when all the acquisitions are performed at two opposite points, located as far as possible from the center **C** of the measured feature (left of figure 7). In this case the standard deviation of a_1 can be written as equation (20).

$$\mathrm{var}(a_1) = \frac{\sigma_p^2}{\sum x_k^2} = \frac{\sigma_p^2}{N.X^2} \Rightarrow \sigma(a1) = \frac{\sigma_p}{X.\sqrt{N}} \tag{20}$$

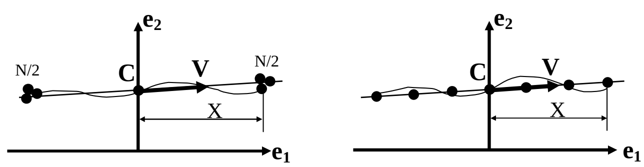

Fig.7. Measured point positions

In that case, however, the variance (σ^2) will no longer integrate the form defect of the surface but only the repeatability of the CMM. This method must thus be used with caution. It should not be used in general, but only applied to standards of perfect geometry, where the form defects are negligible. Many research tasks were undertaken to determine the best distribution of the measured points on the analyzed surface [10], [11]. When the measured points are evenly distributed around the center C; the variance of a_1 is defined by equation (21) (right of figure 7).

$$\text{var}(a_1) = \frac{\sigma_p^2}{\sum x_k^2} = \frac{3.\sigma_p^2}{Q.N.X^2} \text{ with } Q = \frac{2+3.N+N^2}{N^2} \quad (21)$$

The limit of Q is equal to 1 when the N number of points tends to infinity. An acceptable value of Q is obtained when N equals three times the number of parameters. In this case, the standard deviation of the parameter a_1 is calculated by equation (22). The effect of the number of points is less significant than in the other case (equation 20); the size of measured surface has a large influence on the a_1 uncertainty.

$$\sigma(a_1) = \frac{\sigma_p}{X\sqrt{N/3}} \quad (22)$$

It is therefore recommended to acquire points randomly distributed on the surface to avoid any bias introduced by automatic cycles applied to periodic textures. This problem has been illustrated by Weckenmann in one of his papers [12].

3.3. Uncertainty of the distance point / line

Until now, the propagation of the uncertainties of the best fit surface has been studied. A verification of geometrical specifications using the ISO1101 standard without modifier is based on distance calculation. In this paragraph, the verification phase is studied. Its aim will be to calculate the uncertainty of the distance between a point **M** belonging to the specified element and the straight line considered as the datum reference. The factors influencing it will be thus studied.

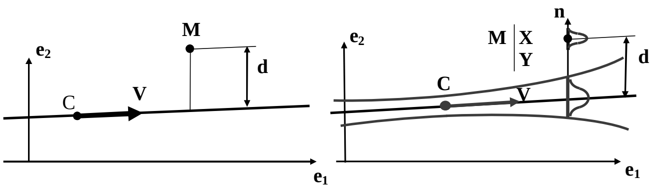

Fig.8. Uncertainty of the d distance

Point **M** is defined by its mean coordinates and a variance which is assume to exist only in direction e_2. These statistical parameters are summarized in equation (23):

$$\mathbf{M}\begin{vmatrix} X \\ Y \end{vmatrix} \quad \text{Cov}(\mathbf{M}) = \begin{pmatrix} 0 & 0 \\ 0 & \text{var}(Y) \end{pmatrix} \quad (23)$$

The datum straight line defined by **C** and **V** in the figure 8 is independent of point **M**. The equation of the distance d between the straight line and the point M is defined by the following equation (24):

$$d = Y - (a_0 + a_1.X) \quad (24)$$

In first time, in order to calculate the distance uncertainty, the Jacobian matrix should be constructed. This matrix is given by equation (25):

$$J = \left[\frac{\partial(d)}{\partial a_0}, \frac{\partial(d)}{\partial a_1}, \frac{\partial(d)}{\partial X}, \frac{\partial(d)}{\partial Y}\right] = \begin{bmatrix} -1 & -X & 0 & 1 \end{bmatrix} \quad (25)$$

In a second time, the variance covariance matrix of the geometrical elements must be built (equation 26):

$$\text{Var}[\text{parameter}] = \begin{pmatrix} \text{var}(a_0) & \text{cov}(a_0, a_1) & 0 & 0 \\ \text{cov}(a_0, a_1) & \text{var}(a_1) & 0 & 0 \\ 0 & 0 & 0 & 0 \\ 0 & 0 & 0 & \text{var}(Y) \end{pmatrix} \quad (26)$$

The uncertainty of the distance d is obtained through the classical Jacobian propagation expression given by equation (27):

$$\begin{aligned} \text{var}(d) &= J.\text{Var}[\text{parameter}].J^t \\ \text{var}(d) &= \text{var}(Y) + \left[\text{var}(a_0) + 2.X.\text{cov}(a_0, a_1) + X^2.\text{var}(a_1)\right] \end{aligned} \quad (27)$$

Equation (27) brings to the fore the great impact of the line uncertainties in the resulting random deviations. The measurement rules defined previously must be employed in the process planning used in measuring the datum reference. To reduce the datum reference uncertainties, the number of measured points and the size of the measured surface must be increased. Using the geometrical description of the surfaces (**C**, **V**), it is possible to propose the procedures to calculate the uncertainties of the 3 classical distances: Point/Point (Pt/Pt), Point/Line (Pt/Dr) and Point/Plane (Pt/Pl). These 3 cases have been summarized in table 2.

Table.2. Uncertainty of the distance PT/PL, PT/DR, PT/PT

	distance Pt/Pl	***distance Pt/Dr***	***distance Pt/Pt***
i: 1 à 3	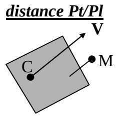	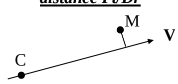	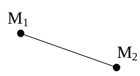
Mean value	$d = \mathbf{CM} \cdot \mathbf{V}$	$d = \lVert \mathbf{CM} \wedge \mathbf{V} \rVert$	$d_i = \lVert \mathbf{M_1M_2} \rVert$
Jacobian matrix J(d)	$[J] = \frac{\partial(\mathbf{CM} \cdot \mathbf{V})}{\partial \mathbf{e}_i}$	$[J] = \frac{\partial(\lVert \mathbf{CM} \wedge \mathbf{V} \rVert)}{\partial \mathbf{e}_i}$	$[J] = \frac{\partial(\lVert \mathbf{M_1M_2} \rVert)}{\partial \mathbf{e}_i}$
Variances Covariances matrix Cov [X]	$\mathbf{Cov}[X] = \begin{bmatrix} \mathbf{Cov}[\mathbf{V},\mathbf{C}] & 0 \\ 0 & \mathbf{Cov}[\mathbf{M}] \end{bmatrix}$		$\mathbf{Cov}[X] = \begin{bmatrix} \mathbf{Cov}[\mathbf{M_1}] & \mathbf{0} \\ \mathbf{0} & \mathbf{Cov}[\mathbf{M_2}] \end{bmatrix}$
Uncertainty d	$U(d_i) = [J].\mathbf{Cov}[X].[J]^T$		

3.4 Effect of geometrical constructions

To acquire the points of the tested surfaces and carry out the accurate constructions which allow calculating and verifying the distance characterizing the geometrical specification, a process planning of the measurement is required. The uncertainties of the best fit element are then propagated by the geometrical constructions used for the measurement [13]. To illustrate this phenomenon, the case of the construction of a 3D line will be considered. The measurement data consists of two sets of points digitized on two circles. The number of measured points is 12 on each circle. The geometrical construction of the 3D line can be obtained by two types of constructions. The first procedure is started by the best fit of the two circles. After, using the calculated centers of these two circles ($\mathbf{C_A}$ and $\mathbf{C_B}$), the 3D line is built ($\mathbf{I_{CACB}}$ and $\mathbf{V_{CACB}}$). Point $\mathbf{I_{CACB}}$ is defined by the middle of $\mathbf{C_A}$ and $\mathbf{C_B}$. The second way consists in concatenating the two sets of measured points thus building a set of points of a cylinder. After this operation, the best fit of a cylinder is performed (**C** and **V**). The constructed line is defined by the cylinder axis. These elements are summarized in figure 9.

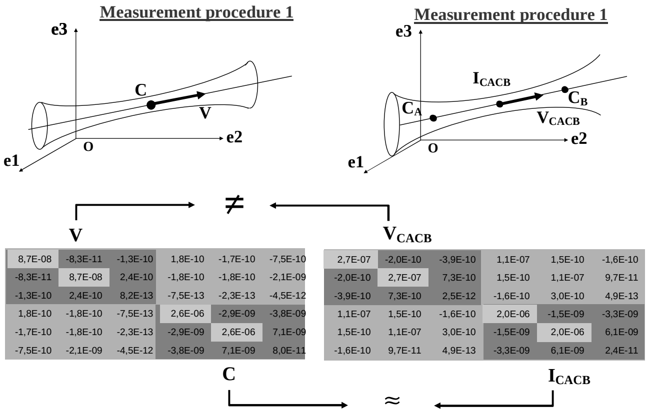

V / C:

8,7E-08	-8,3E-11	-1,3E-10	1,8E-10	-1,7E-10	-7,5E-10
-8,3E-11	8,7E-08	2,4E-10	-1,8E-10	-1,8E-10	-2,1E-09
-1,3E-10	2,4E-10	8,2E-13	-7,5E-13	-2,3E-13	-4,5E-12
1,8E-10	-1,8E-10	-7,5E-13	2,6E-06	-2,9E-09	-3,8E-09
-1,7E-10	-1,8E-10	-2,3E-13	-2,9E-09	2,6E-06	7,1E-09
-7,5E-10	-2,1E-09	-4,5E-12	-3,8E-09	7,1E-09	8,0E-11

V_{CACB} / I_{CACB}:

2,7E-07	-2,0E-10	-3,9E-10	1,1E-07	1,5E-10	-1,6E-10
-2,0E-10	2,7E-07	7,3E-10	1,5E-10	1,1E-07	9,7E-11
-3,9E-10	7,3E-10	2,5E-12	-1,6E-10	3,0E-10	4,9E-13
1,1E-07	1,5E-10	-1,6E-10	2,0E-06	-1,5E-09	-3,3E-09
1,5E-10	1,1E-07	3,0E-10	-1,5E-09	2,0E-06	6,1E-09
-1,6E-10	9,7E-11	4,9E-13	-3,3E-09	6,1E-09	2,4E-11

Fig.9. Comparison of two variances covariances matrix

To measure the effect of the constructions, the variance covariance matrixes of the two procedures are studied. Figure 12 presents the two measurement procedures and the resulting variance covariance matrix. The localization of the center points **C** and $\mathbf{I_{CACB}}$ is similar in the two cases, but the number of points used in the best fits is not the same. In the first procedure, the number of points is just 12 for each circle, but it reaches 24 for the cylinder used in the second construction. In the equation (20), the term X is thus constant but the number N changes. The variances of the coordinates of the center points **C** and $\mathbf{I_{CACB}}$ are thus of similar magnitude, but the variances of the direction vectors **V** of the cylinder axis are significantly lower than those of the vector $\mathbf{V_{CACB}}$ obtained through the first line construction.

4. CONCLUSION

In this paper the effect of the position and number of points used in CMM measurements have been discussed. To simplify the demonstration, the examples of 2D straight line acquisitions and 3D line constructions have been employed for that purpose. It shows that the choice of the localization of the measured points could be optimized using a statistical point of view. Such approach should however be restricted to the analysis of surfaces with small form defect. In general it is recommended to acquire points randomly distributed on the surface to avoid any bias introduced by periodic deviations due to the part's texture.

REFERENCES

[1] V.Srinivasan, "An integrated view of Geometrical Product Specification and Verification", Proceedings of the 7th CIRP Seminar on Computer-Aided Tolerancing, Cachan, France, pp.7-17, April 2001.

[2] J. Dovmark, "New interesting concepts from ISO/TC 213", ACMC Annual General Meeting in Ottawa, Canada, December 3rd, 2001.

[3] A. Weckenmann, J. Lorz, S. Beetz, "Monitoring coordinate measuring machines by user-defined calibrated parts", 9th CIRP Seminar on Computer Aided Tolerancing, Tempe, proceeding on CD Rom, April 2005.

[4] S.D. Antunes, M.A.F. Vicente, "Estimation of precision and uncertainty of a calibration artefact for CMMS", Advanced Mathematical and Computational Tolls in Metrology VI edited by P. Carlini, M.G. Cox & G.B. Rossi, Vol.66, 2004, pp.1-15.

[5] H. Schwenke, B.R.L. Siebert, F. Waldele, H. Kunzmann, "Assessment of uncertainties in dimensional metrology by Monte Carlo simulation. Proposal of a modular and visual software". Annals CIRP vol.49, 395-398; 2000.

[6] T. Kurfess, D. L. Banks," Statistical verification of conformance to geometric tolerance", Computer Aided Design, 1995, Vol.27; pp.353-361.

[7] H.T. Yau, "Evaluation and uncertainty analysis of vectorial tolerances", Precision engineering, 1997, Vol.20; pp.123-137.

[8] K.D. Summerhays, R.P. Henke, J.M. Balwin, J.M.Cassou, C.W. Brown, "Optimizing discrete point sample patterns and measurement data analysis on internal cylindrical surfaces with systematic form deviations", Precision engineering 2002, Vol.26; pp.105-121.

[9] J.R. Taylor, "An introduction to error analysis: The study of the uncertainties in physical measurement", Second edition, University Science Books, ISBN 0935702-75-X; 1997.

[10] P. Bourdet, C. Lartigue, F. Leveaux, "Effects of data point distribution and mathematical model on finding the best fit sphere data", Precision engineering 1993, Vol.15; pp.150-157.

[11] R. Edgeworth and R. G. Wilhelm, "Uncertainty Management for CMM Probe Sampling of Complex Surfaces", ASME Manufacturing Science and Engineering, 1996, Vol.4; pp.511-518.

[12] A.Weckenmann, H.Eitzert, M.Garmer, H.Weber, "Functionality-oriented evaluation and sampling strategy in coordinate metrology", Precision engineering 1995, Vol.17; pp.244-252.

[13] J. Bachmann, J.M. Linares, J.M. Sprauel, P. Bourdet, "Aide in decision making: Contribution to uncertainties in three dimensional measurements", Precision Engineering 2004, Vol.28; pp.78-88.